ELECTROSTATIC THRUSTORS FOR SPACE PROPULSION, PRESENT AND FUTURE*

By WILLIAM R. MICKELSEN†, M.S., A.F.A.I.A.A. and HAROLD R. KAUFMAN‡, B.S., M.A.I.A.A.

(Communication from the National Aeronautics and Space Administration, U.S.A.)

ABSTRACT

Although some existing electrostatic thrustors have sufficient durability for interplanetary flight, shortcomings of these thrustors would incur serious payload losses. It is shown that these shortcomings are especially severe with regard to programmed specific impulse, efficiency, power conversion requirements, and thrustor mass. The detailed status of electrostatic thrustor components is examined on the basis of performance in space missions. The electron-bombardment thrustor appears to be superior to other thrustors at present.

With the thrustor mission-performance analysis as a background, research programmes are described for electron-bombardment thrustors and contact-ionization thrustors. The critical component in the electron-bombardment thrustor is the cathode, and recent data indicate that durable, low-power cathodes can be developed. The performance of the contact-ionization thrustor is severely limited by porous-tungsten technology. The requirements for sub-micron, close-spaced pores without in-flight-sintering appear formidable. Colloidal-particle thrustors are still in the research stage, but appear to have the best promise for high efficiency at low specific impulse, low mass, and programmed specific impulse operation.

I. INTRODUCTION

IT is the purpose of this paper to show the present status of electrostatic thrustors as a component of electric propulsion systems, to describe in detail their major research and development problems, and to discuss their possible future performance.

At present, the chemical rocket is man's only operational primary propulsion system for spaceflight. Nuclear rockets and electric rockets consist only of paper schemes and preliminary experimental equipment. It is clear, however, that if the performance of these propulsion systems lives up to expectations their use will make possible many space missions that are impractical with chemical rockets.

Electric-propulsion systems can be divided into three major parts: the electric powerplant, the thrustor, and any power-conversion equipment between the two. The requirement for electric-propulsion systems with regard to weight and durability has been discussed recently.[1,2] Electric rockets can be competitive in payload fraction with nuclear rockets for Mars missions only if they achieve a specific mass of about 10 kg.kW.$^{-1}$ or less. To be competitive in trip time as well as payload fraction, the electric-propulsion system should be about 5 kg.kW.$^{-1}$ or less.

Most, if not all, of electric-propulsion-system mass is usually assumed to reside in the electric powerplant. Analytical studies[3-9] have resulted in estimates of powerplant masses in the range from 1 to 6 kg.kW.$^{-1}$ The only operational space electric powerplants, however, are solar cells and theremoelectric systems with specific masses from 50 to 100 kg.kW.$^{-1}$—too heavy to match even the small payload fraction of chemical rockets. Reduction of this large gap between actual and required powerplant masses is the aim of a large current research and development programme in the U.S. Since the electric thrustor is useless without a suitably lightweight electric powerplant, it must be assumed herein that this programme will be successful.

The first portion of this paper is devoted to an examination of the present status of electrostatic thrustors with regard to their integration as a component in lightweight propulsion systems. An existing experimental thrustor is used as an example, and the effects of the performance of this thrustor on some space missions are determined.

From this examination, a number of shortcomings of existing thrustors become apparent. Reasons for these shortcomings are explained in terms of the basic physical processes for each of the thrustor types. Research and development programmes on these problems are summarized.

This paper is based on a N.A.S.A. report,[10] which contains considerable additional analysis and discussion.

II. THRUSTOR PERFORMANCE

To illustrate the performance and deficiencies of existing electrostatic thrustors, the theoretical payload capacity of an electric rocket vehicle is shown in Fig. 1 for a one-way Mars orbiter mission starting in a low orbit about Earth and ending in a low orbit about Mars. The powerplant is assumed to have a specific mass of 4 kg.kW.$^{-1}$.
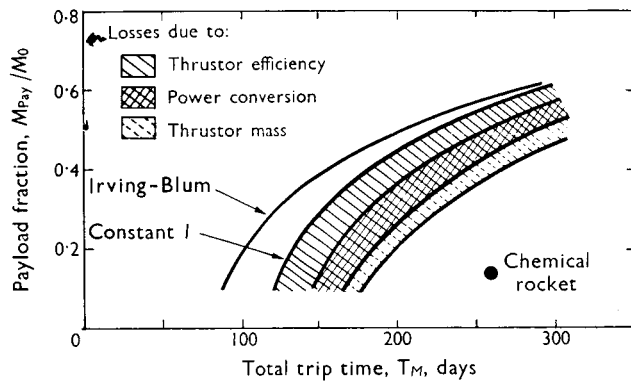
FIG. 1. Payload fraction as a function of trip time for Mars orbiter mission. Basic electric powerplant mass, 4 kg.kW.$^{-1}$ Hatching shows losses due to thrustor efficiency, power conversion, and thrustor mass.

The upper curve in Fig. 1 represents the maximum theoretical payload for the assumption that both the thrustor and the power-conversion equipment have 100% efficiency and negligible mass. In addition, it is assumed that the thrustor is capable of operating with the continuously variable thrust required to maximize the payload during interplanetary transfer.[11] Since the jet power P is maintained constant, the specific impulse I must also vary continuously. The relation between thrust and specific impulse is given by:

$$P_j = \tfrac{1}{2} F g_c I \qquad \text{..} \qquad \text{..} \qquad (1)$$

where the specific impulse is defined as

$$I = \frac{F}{g_c \dot{m}_{\text{tot}}} \qquad \text{..} \qquad \text{..} \qquad (2)$$

F is the thrust, $\dot{m}_{\text{tot}}$ is the propellant mass flow rate, and g_c is the gravitational conversion factor. In the variable-thrust optimized trajectory (Irving–Blum), the specific impulse varies over a large range (*e.g.*, 10:1) with the lowest specific impulse occurring in the planetocentric phases.[11-13] Since existing thrustors are not capable of efficient operation over the required range of specific impulse, an alternative trajectory, using constant specific impulse and thrust, with an optimized coast period in the middle of the heliocentric phase may be used instead. The first loss in payload shown in Fig. 1 is due to use of such constant specific impulse trajectories (this curve was calculated from information in MacKay[14]).

The more advanced electrostatic thrustors require most of their power in the form of high-voltage direct current, while power is generally produced in the form of low-voltage alternating current. The power could, of course, be generated as high-voltage alternating current, so that only rectification is necessary. But a recent analysis[15] of power-conversion equipment in the 1000-kW. power range has shown that conventional low-voltage electromagnetic generators with transformers should have lower specific mass than

high-voltage electrogenerators without transformers for potential above 2400 V. Since almost all thrustors require potentials higher than 2400 V in the specific impulse range of interest, the high-voltage electromagnetic generator will not be considered further here. Information elsewhere[16] indicates that an electromagnetic generator power-conversion system might be developed from present technology with a specific mass of about 6 or 7 kg.kW.$^{-1}$ for the 1 to 10 MW. power level. With advanced technology, analysis[15] predicts a specific mass of about 1·4 kg.kW.$^{-1}$. This latter estimate was used to calculate the reduction in payload due to power-conversion equipment in Fig. 1. An efficiency of 90% was assumed for this equipment.

Power losses and propellant loss in the thrustor may also seriously reduce the payload capacity. As shown elsewhere,[10] the thrustor efficiency η is

$$\eta \equiv \frac{\tfrac{1}{2} F^2 / \dot{m}_{\text{tot}}}{P} \qquad \text{..} \qquad \text{..} \qquad (3)$$

where P is the total input power to the thrustor. If some of the propellant is not ionized and accelerated, the efficiency may be written as

$$\eta = \left(\frac{\dot{m}_+}{\dot{m}_{\text{tot}}} \right) \frac{F^2}{2 \dot{m}_+ P} \qquad \text{..} \qquad \text{..} \qquad (4)$$

where m^+ is the propellant that is ionized and accelerated (for simplicity only singly charged propellant particles are considered here). A propellant utilization efficiency may be defined that accounts for the propellant loss:

$$\eta_U \equiv \frac{\dot{m}_+}{\dot{m}_{\text{tot}}} \qquad \text{..} \qquad \text{..} \qquad (5)$$

and a power efficiency may be defined that accounts for electric power loss:

$$\eta_P \equiv \frac{F^2}{2 \dot{m}_+ P} \qquad \text{..} \qquad \text{..} \qquad (6)$$

From these definitions the thrustor efficiency is

$$\eta = \eta_U \eta_P \qquad \text{..} \qquad \text{..} \qquad (7)$$

The efficiency of an existing Lewis electron-bombardment thrustor has been used to illustrate the effect of current thrustor inefficiencies on payload capacity in Fig. 1.

The mass of thrustors can also reduce payload capability. This mass is strongly dependent on specific impulse and durability requirements. The mass of existing thrustors is a substantial fraction of the payload mass, as illustrated in Fig. 1. The reduction in payload shown in Fig. 1 is based on extrapolation of durability test data (to be discussed later) for the current Lewis electron-bombardment thrustor. The optimization procedure used is described elsewhere.[10]

From Fig. 1, it is evident that existing thrustors would cause considerable loss in payload or trip time due to thrustor inefficiency, thrustor mass, and operation at constant specific impulse. Power-conversion systems,

even of an advanced design, would also cause much payload loss. The net result of these losses is equivalent to an increase in overall specific mass from the assumed powerplant value 4 kg.kW.$^{-1}$ to about 10 to 15 kg.kW.$^{-1}$. Further calculations[10] show that existing thrustors would cause even greater relative loss in payload capacity for Mars round-trip vehicles. Although spaceflight is possible with existing thrustors, the potential gains in payload capacity warrant a critical examination of the various electrostatic thrustor-design concepts with regard to their possible improvement and ultimate performance.

III. ELECTROSTATIC THRUSTOR PRINCIPLES

In the electron-bombardment thrustor, propellent atoms or molecules are ionized by electron impact. A plasma results in the ionization chamber. The ions are extracted from the plasma by virtue of the electric field in the accelerator. Propellents of interest in present electron-bombardment thrustors are caesium, mercury and heavy molecules (mass greater than 200 amu*).

In the contact-ionization thrustor, atoms are ionized by surface contact of a low-ionization-potential atom on a high-work-function surface. The surface is hot, so that the ions are evaporated, after which they are accelerated by the electric field of the accelerator. The combination of most interest is caesium as the propellent and tungsten as the surface.

The colloidal-particle thrustor is still in a state of basic and applied research. There are a number of schemes for particle generation and charging, which will be discussed in later sections. Propellent mass-to-charge ratios of less than 100,000 amu per electronic charge are of interest.

All these thrustors produce thrust with the same basic principle, which is the acceleration of charged particles in an electric field, as indicated in Fig. 2. Electrons removed from the propellent particles are drawn from
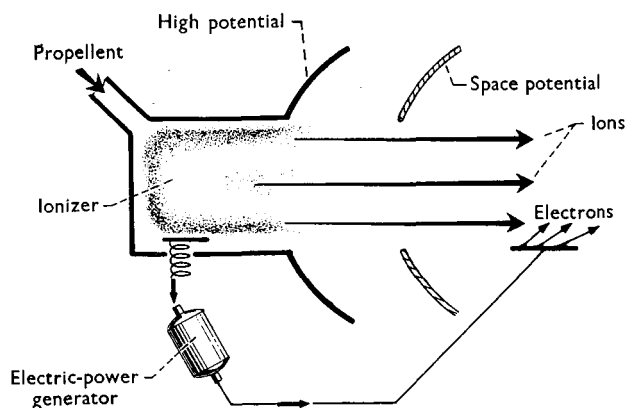
the high-potential charging chamber, or ionizer, by the electric powerplant and are injected into the charged-particle exhaust. The charged particles merely fall through the potential difference to obtain the desired exhaust velocity.

It is essential that the charged-particle exhaust be neutralized, particularly since the accelerator is at or near space-charge-limited current density.[17,18] This neutralization requires: (1) equal rates for the ejection of opposite charges (current neutralization) to avoid building up a large charge on the space vehicle, and (2) equal densities of opposite charges in the beam (charge neutralization) to avoid large space-charge effects within the beam. Early theoretical analyses predicted that beam neutralization would be a serious problem; however, early experimental operation in vacuum facilities indicated that the exhaust beams were in fact neutralized.[19] In a series of definitive experiments, Sellen and Kemp[20] showed that ion beams up to 10 ft. in length could be neutralized under closely simulated free-space conditions. From these experiments, it appears that beam neutralization will not be a fundamental problem. To obtain absolute verification, beam neutralization will be tested in the SERT-1 spaceflights.[21]

The remaining neutralization problem appears to be the development of durable neutralizers. The electron emitter should be only a few volts below the potential of the neutralized beam. Because of space-charge limitations on electron current, it is necessary to have a very short distance between the electron emitter and the ion beam if the electron emitter is to have a reasonably small size. If the edge of the ion beam were sharply defined, the neutralizer could simply be brought up close to the edge of the beam. Even if the ion optics were good enough to make a sharply defined beam edge, charge-exchange ions would probably make some sort of shadow shielding necessary for long-life neutralizers.

An estimated life of 25 hr. was obtained for one of the shielded configurations investigated.[22] This short lifetime was probably the result of charge-exchange ions formed near the neutralizer. Since the potential difference between the neutralizer and the exhaust-beam plasma was over 50 V. for this configuration, these charge-exchange ions were sufficiently energetic to cause considerable sputtering erosion. A better shielded-neutralizer design with only a 10- to 20-V. potential difference between it and the beam should have no trouble reaching any desired lifetime. Since the neutralizer does not appear to offer any major problems and since neutralization problems are substantially similar for all types of thrustors, they will not be considered further. It is true that a colloidal-particle thrustor may require a supply of protons rather than electrons, but such a neutralizer should still be a minor problem compared to the rest of the thrustor.

High potential

Propellent

Space potential

Ions

Ionizer

Electrons

Electric-power generator

Fig. 2. Schematic diagram of electrostatic thrustor.

* Atomic mass units.

IV. THE ELECTRON-BOMBARDMENT THRUSTOR

A typical electron-bombardment thrustor is shown in Fig. 3. Energetic electrons, contained by electric and magnetic fields, are used to ionize atoms in this thrustor.
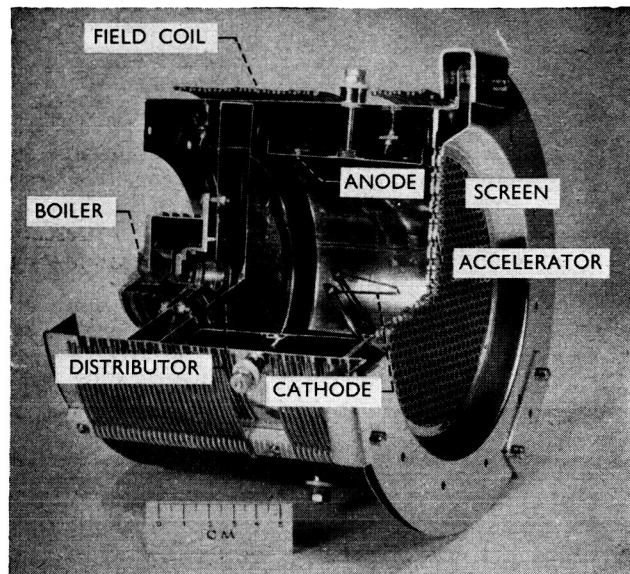

FIG. 3. Electron-bombardment thrustor for mercury propellent.

Production of ions by electron bombardment is not a new concept. But previous electron-bombardment ion sources that produced sufficient ion current to be of interest for electric propulsion (such as that of Von Ardenne[23] had current densities too high to be transmitted by practical accelerator systems. The contribution of Kaufman and Reader[24,25] was primarily an electron-bombardment ion source that matched the current-density requirements of a long-life electrostatic accelerator system operated in the specific impulse range of interest.

The performance of electron-bombardment thrustors obtained in the initial investigations showed substantial advantages as compared with other ion thrustors of that period.[26] Because of these advantages, a sustained research programme on this type of thrustor has been conducted at the N.A.S.A. Lewis Research Center. More recently, contractual work with private industry[27-29] has augmented the work at Lewis.

The propellent is vaporized and passes through the distributor into the ion chamber. In the ion chamber it is bombarded by electrons from the cathode. The collisions of electrons with the propellent atoms are enhanced by an axial magnetic field, which prevents the rapid escape of electrons to the anode. Escape of electrons to the ends of the ion chamber is prevented by operating these ends at the same potential as the cathode. Some of the propellent becomes ionized by the bombardment of electrons, and some of these ions arrive at the screen and are accelerated into the ion

beam (the ions that are not accelerated into the ion beam recombine with electrons at the walls of the ion chamber). An electron source (not shown in Fig. 3) then neutralizes this ion beam.

The problem areas of this type of thrustor can be divided into those of the ion chamber, the magnetic field, the cathode, and the accelerator. These problem areas will be discussed in this order in the following sections.

1. ION CHAMBER

Following the initial studies,[24,25] an extended investigation[30] was conducted to determine optimum ion-chamber geometry. The optimum of the cylindrical ion-chamber geometries investigated was a length approximately equal to the diameter, and the anode length nearly equal to ion-chamber length. Some optimization of distributor design was found desirable for each combination of current density and specific impulse. The ion chamber was otherwise found to be insensitive to small changes in geometry, and after extended testing, the optimum geometry did not differ greatly from the best geometry reported by Kaufman and Reader.[24] The discharge power, approximately the cathode emission times the ion-chamber potential difference, is shown as energy per beam ion in Fig. 4
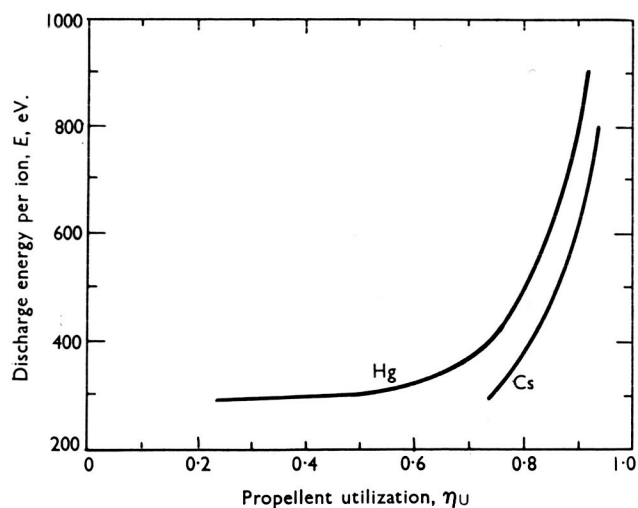

FIG. 4. Ion-chamber losses as a function of propellent utilization.

for mercury propellent and a good geometry. Some development is required to obtain this level of performance, but it has been obtained many times—and frequently exceeded. In addition to changing the distributor, the accelerator geometry may also have to be changed, as discussed in Section IV.4.

The standard operating conditions employed[24,25,30] included a 50-V. potential difference between the anode and cathode in the ion chamber. With this potential difference, it was found[31] that 5–10% of the ions leaving

the ion chamber were doubly ionized, which would correspond to a thrust loss of 1·5–3% and an efficiency loss twice as large. Dropping the ion-chamber potential difference to 30 V. had little effect on the discharge energy per beam ion, but the percentage of doubly ionized ions was found to decrease to 2–5%. This reduction in potential difference also had the beneficial effect of reducing cathode sputtering.

Cæsium has been investigated as a propellent for an electron-bombardment thrustor designed by Speiser[27] and shown in Fig. 5. The results indicate that a somewhat
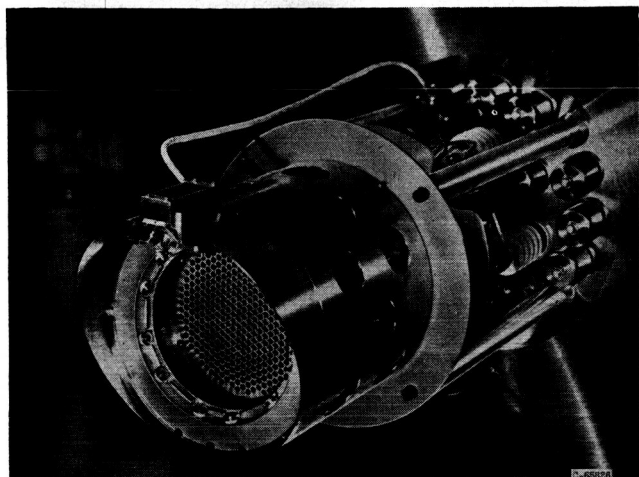

FIG. 5. Electron-bombardment thrustor designed at Electro-Optical Systems, Inc., for cæsium propellent.

lower discharge energy per beam ion can be expected with cæsium as the propellent (as indicated by the second curve in Fig. 4). Even with the lower discharge power, though, the lower atomic weight of cæsium (132·9 *versus* 200·6 for mercury) would result in lower thrustor efficiencies unless additional power savings were made elsewhere. As will be discussed in Section IV.3, such additional power savings are possible.

Propellents with even heavier atomic weights than mercury would be desirable for improving both the efficiency and thrust density of an electron-bombardment thrustor at low specific impulses. Since prospective propellents do not exist as atomic species much heavier than mercury, heavy molecules appear to be the only practical substitute. An investigation of possible heavy-molecule propellents is being conducted at Lewis.[32] Complete results have not yet been reported, but considerable experimental work has been completed. Preliminary analysis of the data indicates that molecules substantially heavier than mercury can be ionized and accelerated into a beam, but only for propellent utilizations less than 10%. The mean molecular weight is reduced, owing to fragmentation at higher utilizations. Further experiments are planned, but the simultaneous achievement of high utilization and high mean molecular weight does not appear likely.

Some improvement in ion-chamber performance might be obtained through ion-chamber accelerator interactions, as is discussed in Section IV.4. It is felt, though, that near-optimum geometry has already been obtained for the ion chamber and that further improvements would be small and difficult to achieve.

No problems were encountered concerning durability in the ion chamber (with the exception of the cathode, which is treated separately) even though material as thin as 0·2 or 0·3 mm. was used for various parts.

2. MAGNETIC FIELD

The problem that has been associated with the magnetic field in the past has been a compromise between mass and power. Solenoidal windings on research thrustors, where mass is unimportant, can be quite heavy and have correspondingly low power losses. Such windings may weigh as much as 10 lb. for a thrustor with a 10-cm-diameter beam, and have only a 50-W. power loss. On the other hand, a flight-type thrustor may have a field winding that weighs only 1 lb. but has a power requirement of 200 W.

A recent paper[33] indicates a solution to the power *versus* mass problem. The permanent-magnet design investigated therein[33] has a mild-steel distributor plate and screen, with permanent magnets positioned between the two, and this thrustor is shown in Fig. 6. As has been demonstrated,[30] ion-chamber performance is improved when the field strength at the screen is less than that at the distributor. The disparity in sizes of the two pole pieces (distributor and screen) shown in Fig. 6 is the one means of obtaining this field strength difference.
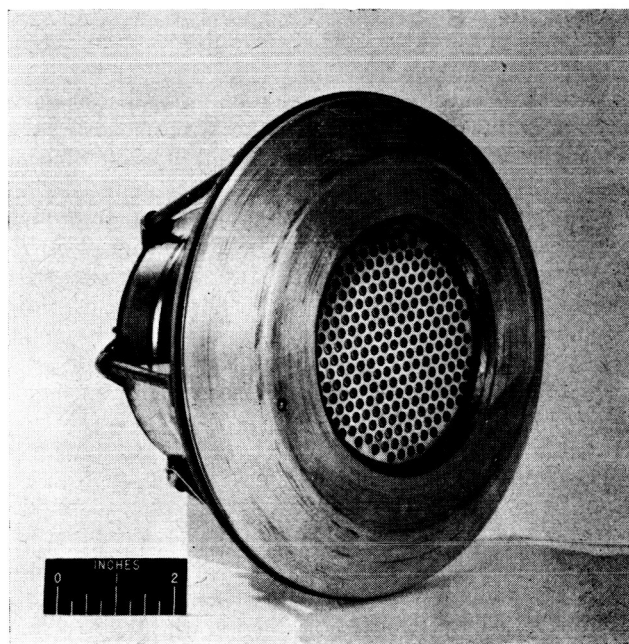

FIG. 6. Permanent-magnet 10-cm. module of electron-bombardment thrustor designed at the N.A.S.A. Lewis Laboratory for mercury propellent.

Except that no field power was required, the permanet-magnet electron-bombardment thrustor operated in a normal manner. Extended operation and cycling conducted since the paper mentioned[33] was published has resulted in no significant change in magnetic field strength. The only adverse results are a lack of operating flexibility (which is of interest mainly in research) and decreased thermal-structural stability of the mild-steel screen as compared to the molybdenum screen it replaced. More careful design for thermal-expansion effects should solve this latter problem.

One of the most important virtues of the permanent-magnet design[33] is its low mass. The total mass of the permanent-magnet thrustor is 3 lb., which is almost exactly that of a flight-type thrustor of the same size (10-cm.-dia. beam) that employed a high-loss, low-weight solenoidal winding.

3. CATHODE

Both power and lifetime problems are associated with the cathode. The early electron-bombardment thrustor experiments at the Lewis laboratory were conducted with tantalum, and occasionally tungsten, cathodes. Although pure tantalum has severe power and durability problems, it is very easy to use and gives reproducible results. A desired lifetime with tantalum is achieved simply by supplying sufficient cathode material to offset sublimation and erosion. From tests with tantalum strips at Lewis,[34] it appears possible to use tantalum for attitude-control thrustors where the actual operating time may only be 1000 to 2000 hr., and efficiency is not of primary importance. For main propulsion systems, with anticipated lifetimes of perhaps 10,000 hr., tantalum cathodes are out of the question. Tungsten, with electron-emission characteristics similar to tantalum, would also be unacceptable.

A more promising type of cathode uses alkaline-earth carbonates in a compositive structure with nickel or some other relatively inert metal. The metal provides a structural matrix to hold more of the emitter material than could be applied with just a coating on the outer surface. A nickel-matrix cathode[28] was operated in an electron-bombardment thrustor designed at Ion Physics Corporation (Fig. 7) for periods up to 300 hr. Investigations have been conducted at Lewis with another type of metal-matrix cathode. One test at Lewis in a simulated thrustor (a complete thrustor except for the accelerator) had a duration of more than 1600 hr. The heater power increased with time, going from about 15 to 30 W. per emitted ampere at the end of 1600 hr. The performance obtained to date indicates that good efficiency for a 10,000-hr. life may be possible with this type of cathode.

The final type of cathode to be considered is the auto-cathode shown in Fig. 8 which is being developed by Electro-Optical Systems in conjunction with the electron-bombardment thrustor of their design[27] (Fig. 5). Use of cæsium propellent to provide a low work function emitter surface and ion bombardment for heating it
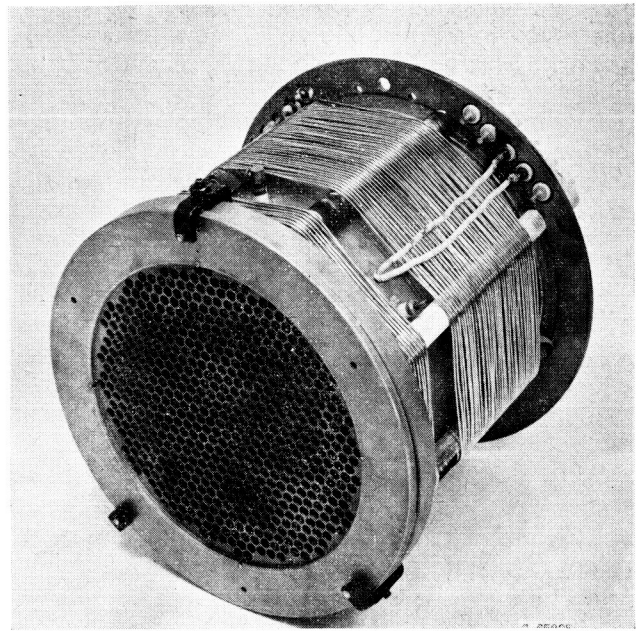

FIG. 7. Electron-bombardment thrustor designed at Ion Physics Corp.

results in a long-life cathode that requires no heating power. The ion-chamber potential difference with cæsium as the propellent can be sufficiently low so that cathode sputtering is not a problem, and the temperature of a cæsium-coated cathode can be so low that sublimation of the base metal should be negligible. Thus, there should be no major obstacle to the attainment of a 10,000-hr. lifetime, or even longer, with this type of cathode. The major shortcoming is the increased charge-exchange cross section of cæsium, which serves to limit the thrust-to-area ratio of the accelerator.

The ion chamber, the magnetic field, and the cathode, just discussed, are the major loss sources in a well-designed electron-bombardment thrustor. A good estimate of the performance that can be expected with mercury as the propellent is obtained by selecting an electron emitter loss of 20 W. per emitted ampere, a
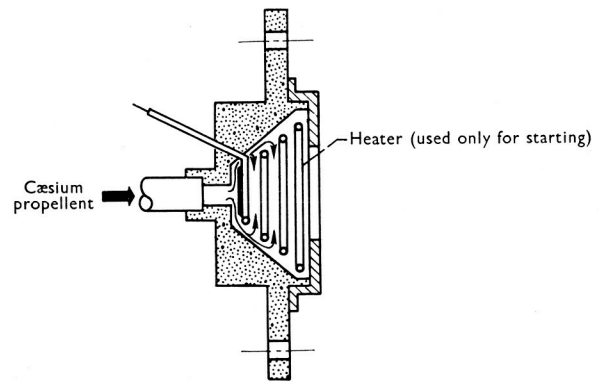

FIG. 8. Diagram of cæsium autocathode.

30-V. ion-chamber discharge, and the discharge losses quoted in Section IV.1. An additional 1% jet-thrust may be assumed for impingement and off-axis velocity effects. The performance calculated with these assumptions has been presented[35] and is shown in Fig. 9. A trade-off can be made between ion-chamber and propellent-utilization losses. The optimum utilization (for efficiency) is also shown in Fig. 9. Although a minimum power-to-thrust ratio of about 100 kW.lb$_f$.$^{-1}$ is shown in Fig. 9, operation below about 4000 sec. is difficult because of accelerator current-density limitations. A power-to-thrust ratio of about 150 kW.lb$_f$.$^{-1}$ would therefore be a more realistic lower limit. Similar calculations were made for cæsium as the propellent. The assumptions were the same except that the lower discharge losses of cæsium were used, and a 20-V. discharge was assumed. A small cathode power loss of 5 W. per emitted ampere was assumed so that better control of the discharge could be obtained than with an auto-cathode. The optimum efficiency obtained with cæsium was about 1% higher than that shown in Fig. 9. The optimum utilization was also increased 1 to 2% over that of Fig. 9. Although the curves of Fig. 9 are
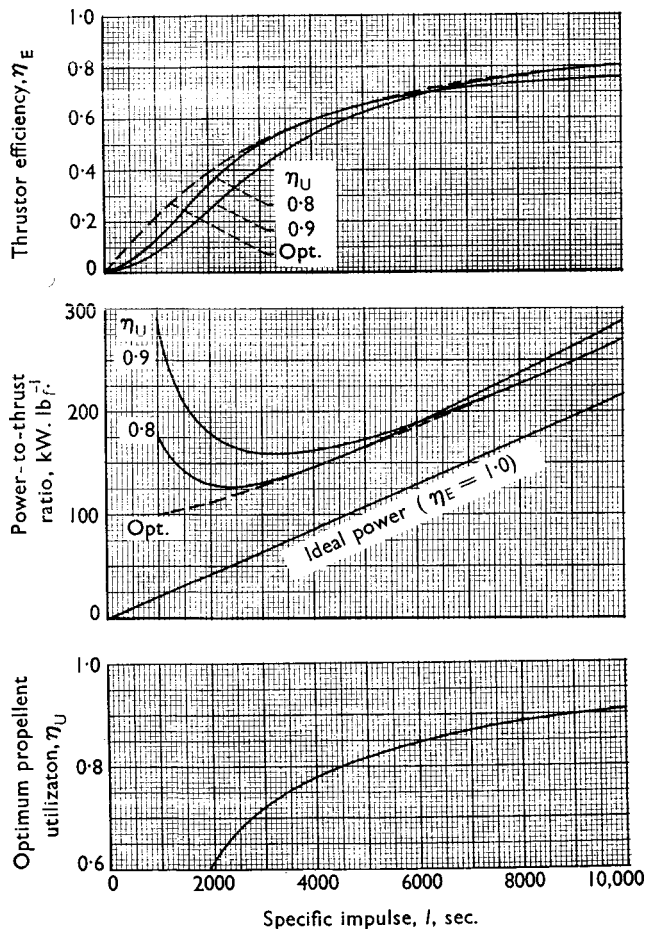
calculated, experimental values within a few per cent of the maximum efficiency curve have been obtained over a wide range of specific impulse.

4. ACCELERATOR

The problem posed by the accelerator is primarily one of durability. A thorough study of accelerator configurations for the electron-bombardment thrustor was conducted at Lewis and has been decribed.[36,37] As shown,[36] operation well below space-charge limitations with a carefully aligned accelerator system can result in impingement currents approaching that from charge exchange alone. Later tests at Lewis[38] have verified this conclusion. With mercury as the propellent, the ion-impingment and accelerator-drain current are substantially equal. The measurement of ion impingement with mercury is therefore much simpler than with cæsium.

As has been shown,[38] the accelerating system of existing thrustors with 10-cm.-dia. beams should last 10,000 hr. at a specific impulse of 4000 sec. and a propellent utilization of 76% if the current of mercury ions does not exceed about 0·13 A. This lifetime corresponds to a total ion impingment of 3·3 A.hr., which is sufficient to erode through the thinnest sections of the accelerator. The variation of lifetime L with ion-beam current and propellent utilization is of the form

$$L \propto \frac{\eta_U}{1 - \eta_U} \frac{1}{J_B^2} \qquad \qquad (8)$$

when charge exchange is assumed to be the primary cause of accelerator impingement. The effect of specific impulse on lifetime is also of interest. However, since different combinations of net accelerating potential difference Φ_{net} and propellent utilization can yield the same specific impulse, the ion energy (and hence sputtering damage) therefore does not have a unique relation with specific impulse. A working relation for the effect of specific impulse may be obtained by assuming utilizations near the optimum for efficiency, as shown in Fig. 9. The lifetime proportionality thereby obtained is

$$L \propto \frac{\eta_U}{1 - \eta_U} \frac{1}{J_B^2} \left(\frac{4000}{I}\right)^{1·13} \qquad \qquad (9)$$

Using the lifetime data at 4000 sec. from Kerslake[38] for a 10-cm. beam thrustor yields a constant of proportionality. The maximum ion current for this size thrustor is thus:

$$J_B = \left[\frac{2·23}{L}\left(\frac{\eta_U}{1 - \eta_U}\right)\left(\frac{4000}{I}\right)^{1·13}\right]^{1/2} \qquad (10)$$

with L the lifetime in days. This equation, together with an actual single module mass of 3 lb., was used to calculate the mass figures for an electron-bombardment thrustor shown in Fig. 10. Fig. 9 and 10 were used for the calculations of Fig. 1. Any desired lifetime can be obtained simply by reducing the ion-beam current
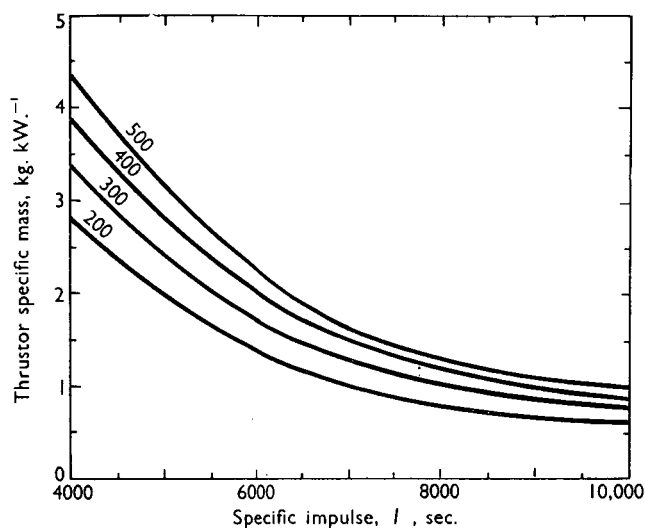

FIG. 9. Estimated performance of electron-bombardment thrustor with mercury propellent.

FIG. 10. Specific mass of electron-bombardment thrustor assuming adequate cathode durability (based on exhaust jet power). Numbers on curves: thrustor durability, days.

to a small enough value. The efficiency of an electron-bombardment thrustor, unlike that of a contact-ionization thrustor, is substantially independent of current density. The only adverse effect of lowering the ion current density is the increased size, and hence weight, of the thrustors.

The effect on the accelerator lifetime of changing the propellent to caesium can be estimated by comparing charge-exchange cross sections and atom:ion sputtering ratios for caesium and mercury.[38–40] The charge-exchange cross section for caesium is two to three times as large as that for mercury. The effect of the larger charge-exchange cross section for caesium, though, is almost balanced by a reduced sputtering (using molybdenum for both). If it is assumed that these two factors balance, the only effect left would be that of charge-to-mass ratio and spacing of the accelerator. Since the acceleration voltage for a given specific impulse will be less with caesium, closer accelerator spacings might be expected with caesium, which would lead to reduced charge-exchange impingement. However, the thrustor mass is greatest at low specific impulses, where the same minimum accelerator spacing (determined by fabrication and structural stability considerations) will probably be used for both caesium and mercury. Thus, although the use of caesium gives the best prospects of a long-life cathode, it will probably cause substantial increases in thrustor mass at low specific impulses. For the same accelerator spacing, the thrust per unit area with caesium would only be about two-thirds that with mercury.

The final topic for the accelerator section concerns the interaction with the ion chamber. The data for the various acelerator configurations investigated elsewhere[36] show substantial effects of accelerator configuration on ion-chamber performance. In general, increasing the

percentage of open area in the screens, reducing the screen thickness, and increasing the accelerating potential difference resulted in lower ion-chamber discharge power loss. One aspect is certainly the loss of ions due to collision on the screen. Changing the variables in the direction indicated will tend to reduce these collisions. It is difficult, though, to explain all of the observed interactions in terms of ion-screen collisions. The electric field from the accelerator system apparently can influence ion motion in a substantial portion of the ion chamber, far more, for example, than would be indicated by a calculation of Debye shielding distance (less than 0·1 mm.). In any event, the accelerator configuration can have a substantial effect on ion-chamber performance. This effect should be considered when trying to optimize performance.

As may be surmised from the preceding discussion, several areas of research on the electron-bombardment thrustor appear to be reaching completion. The ion-chamber configuration, magnetic-field design, and the accelerator structure all fall into this category. A possible exception might be an attempt to produce more uniform current density, which would permit considerably greater power densities for the same lifetime.

The cathode is probably the most important remaining component research area. The caesium autocathode[27] is one promising solution. As was pointed out, however, the use of caesium places more severe limits on the thrust-to-area ratio at low impulse than does mercury. This effect alone is sufficient reason to continue research on alkaline-earth carbonate cathodes, particularly since very substantial lifetimes have already been obtained. Another reason for continuing research on the alkaline-earth carbonate cathode is the possible use of other propellents to obtain variable specific impulse operation.

V. CONTACT-IONIZATION THRUSTORS

The basic concept of the contact-ionization electrostatic thrustor was presented by Stuhlinger[41,42] in 1954. Since the beginning of active experimental work on electric thrustors in 1957–58, the major share of research and development has been devoted to the contact-ionization thrustor.

The distinguishing feature of this thrustor is the method of ionization of propellent atoms. Stuhlinger noted that alkali metal atoms such as caesium could be ionized with high probability on surfaces with high work functions such as tungsten and then could be accelerated with an electrostatic field, as indicated in Fig. 11. The early work on the contact-ionization process by Irving Langmuir, Becker, and others showed that the caesium–tungsten system provided ionization probabilities as high as 99%. In order to preserve the high work function, however, it was necessary to allow only a small fraction of a caesium monolayer on the tungsten surface. This was accomplished by maintaining the tungsten surface at a high temperature (1300° to 1500° K.).
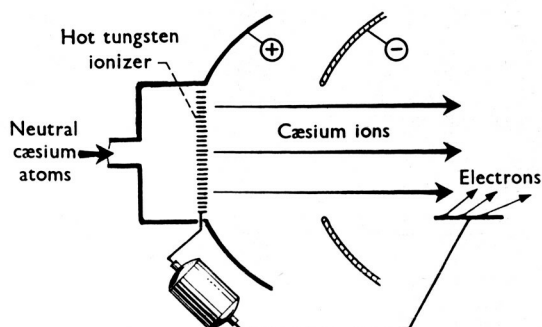
FIG. 11. Schematic diagram of contact-ionization thrustor.

The high temperature causes a considerable thermal-radiation loss, thereby reducing the thrustor efficiency (by increasing the power P) as shown by Eqn. (3). To obtain a reasonable efficiency, a high ion-beam power per unit area must be attained. Ion-beam density may be limited by minimum practical accel distances. For a fixed accel distance, cæsium provides a higher exhaust-beam power density than the other alkali metal atoms by virtue of its highest mass.

For the reasons of highest ionization probability and highest beam power density, the cæsium–tungsten system has been generally accepted as the best for the contact-ionization thrustor. From such optimistic beginnings, contact-ionization thrustors have progressed through much research and development and stand today as nearly flight-worthy devices.

One type of contact-ionization thrustor is under development at Electro-Optical Systems. The progress and performance of this thrustor have been described[43-48] and one of the design versions is shown in Fig. 12. Another type of contact-ionization thrustor is under development at Hughes Research Laboratory. The progress and performance of this thrustor have been described,[49-53] and one of the design versions is shown in Fig. 13.

Both of these thrustors are based on common fundamentals, so they will be discussed concurrently. Both have porous tungsten ionizers. By virtue of its own vapour pressure, cæsium diffuses through the pores of the ionizer and is ionized by contact on the "downstream" face of the ionizer. The cæsium ions are then accelerated by the accelerator elctrodes. The cæsium ions are singly charged, so their final speed is uniform.

The major power loss in these thrustors is due to thermal radiation from the ionizer. Conduction heat loss has been minimized, and the "upstream" side of the ionizer and propellent-feed manifolds are well insulated to minimize thermal-radiation loss. The accel length has been made as short as is now possible and is only a few millimetres in both thrustor concepts.

As shown in Figs. 12 and 13, the EOS thrustor consists of an array of ionizer "buttons" and circular electrode
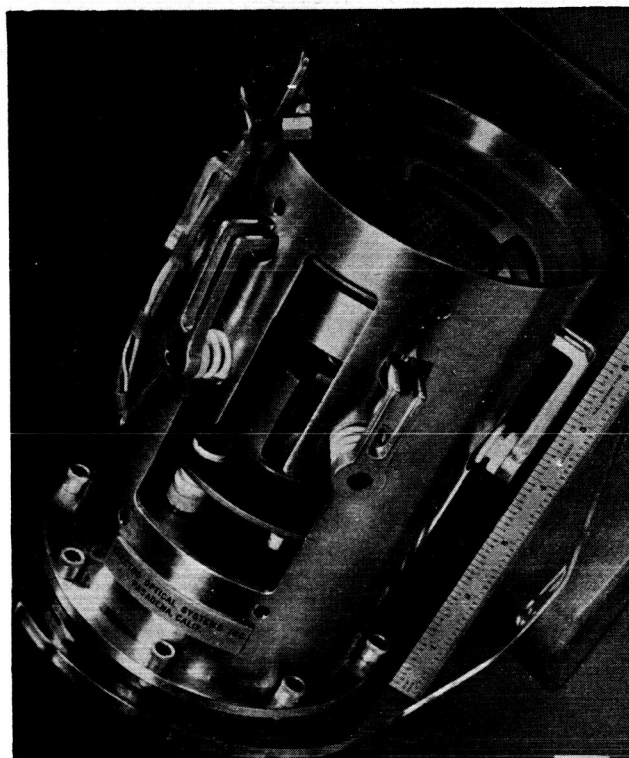

FIG. 12. Contact-ionization thrustor designed at Electro-Optical Systems, Inc.

apertures, while the Hughes thrustor consists of concentric "annular" ionizers and exhaust apertures. Both thrustors have concave ionizer surfaces but different electrode shapes. The neutralizer designs are also different.
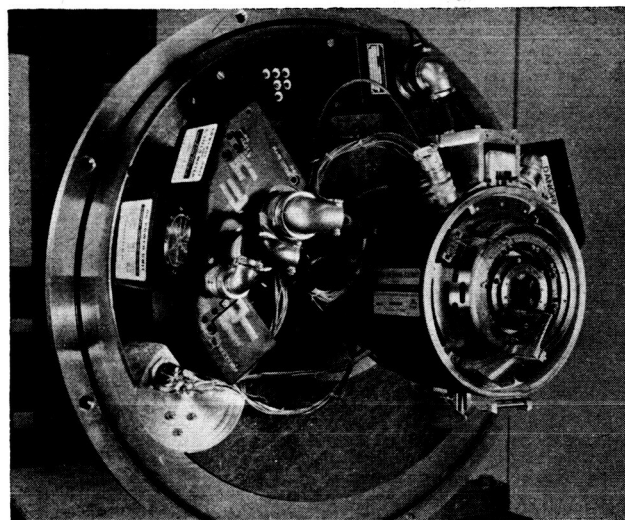

FIG. 13. Contact-ionization thrustor designed at Hughes Research Laboratory.

1. ION OPTICS

Inasmuch as the ions come from a physical surface in the contact-ionization thrustor (as opposed to a diffuse plasma in the electron-bombardment thrustor), the boundary values for the acceleration process can be well defined. A variety of theoretical methods of predicting ion trajectories therefore can be and have been used. Analytic solutions have been summarized[54] and numerical methods of solution given[55,56] by Hamza and co-workers. An electrolytic-tank analogue computer has been a standard design tool at Hughes. The rubber-sheet analogue has also been used in various places but is limited in usefulness due to the impracticality of space-charge simulation.

Theoretical solutions to the acceleration process are of greater importance for the contact-ionization thrustor, than for the electron-bombardment thrustor. Direct impingement of primary ions is masked not only by impingement of charge-exchange ions but by electron emission (both secondary and thermionic) from the accel electrode. It is known that the drain currents from the accel electrode[57] may be as high as 15% of the ion-beam current at ion current densities of 250 A.m.$^{-2}$. A recent theoretical analysis[58] shows that thermionic electron-emission currents from the accel electrode may be very high fractions of the caesium ion current. Neutral caesium atoms from the ionizer can form a layer on the accel electrode, thereby producing a low-work-function surface and resulting in high electron-emission currents. The analysis predicts that either cooling or heating the accel electrode a few hundred degrees Kelvin will reduce the electron-emission current to a negligible level.

Both the EOS and Hughes thrustors are believed to have satisfactory ion optics. In both thrustors, the ion beam is slightly "overfocussed" so that the edge of the beam is a finite distance from the accel and decel electrodes. This separation distance eases design and fabrication tolerances and reduces the effect of ion thermal velocities to a negligible level.

Computer solutions for space-charge-flow geometries such as the EOS and Hughes thrustors show that a considerable variation of ion current density may occur across the ionizer surface[57] without excessive impingement. Non-uniform current density, though, may have other consequences, to be discussed later.

2. CHARGE EXCHANGE

Although the caesium–tungsten system has a very low emission rate of neutral caesium atoms under ideal conditions, this emission is not negligible. Optimization of efficiency requires that maximum current and power densities be used. The optimum is, of course, the highest current density that is consistent with lifetime requirements. As was mentioned in the preceding section, measurement of ion impingement is complicated by electron emission from the accelerator electrode. The erosion effects of charge-exchange ions must therefore

be determined either from actual lifetime tests or from theoretical studies.

A theoretical study at Hughes with the electrolytic-tank analogue computer showed that charge exchange in only a portion of the region near the electrodes contributes to charge-exchange impingement.[29] The region that produces charge-exchange interception for a particular electrode configuration is shown in Fig. 14.
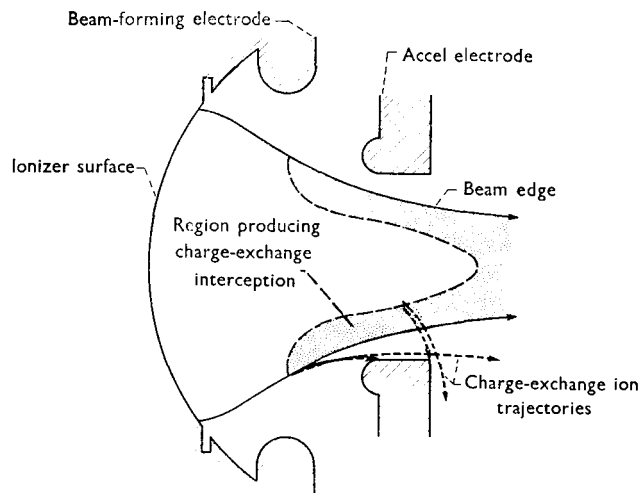

Fig. 14. Theoretical analysis of charge-exchange ion trajectories.

The durability of the EOS and Hughes thrustors has not been fully established on either a theoretical or an experimental basis. It is nevertheless of interest to estimate the durability of their electrodes with the data obtained for the bombardment thrustor.[38] If it is assumed that equal amounts of accelerator electrode material erosion are allowable in caesium and mercury thrustors, that the volume of the charge-exchange region and the accelerator designs are the same, and that the charge-exchange cross sections are $\sigma_{Hg} = 6 \times 10^{-15}$ cm.^{2} (Kerslake[38]) and $\sigma_{Cs} = 2 \times 10^{-14}$ cm.^{2} (Speiser and Vernon[34]), then the ratio of allowable current densities is:

$$\left(\frac{j_{Cs}}{j_{Hg}}\right)_\Phi = 0.55 \left(\frac{Y_{Hg}}{Y_{Cs}}\right)^{0.5} \left(\frac{1 - \eta_U}{\eta_U}\right)^{0.5}_{Hg} \left(\frac{\eta_U}{1 - \eta_U}\right)^{0.5}_{Cs} \quad (11)$$

The sputtering yield for mercury[33] is $Y_{Hg} = 1.5$ atoms per ion for 5000 eV.Hg$^+$ incident on molybdenum. The EOS thrustor has copper accel electrodes, so that sputtered atoms of copper cannot contaminate the ionizer (the melting point of copper is less than the ionizer operating temperature). From Speiser and Vernon,[39] $Y_{Cs} = 6$ atoms per ion for 5000 eV.Cs$^+$ incident on copper. For the same accel potential Φ_A and assuming that Y_{Hg} and Y_{Cs} are both proportional to $\Phi_A^{0.7}$,

$$\left(\frac{j_{Cs}}{j_{Hg}}\right)_\Phi = 0.27 \left(\frac{1 - \eta_U}{\eta_U}\right)^{0.5} \left(\frac{\eta_U}{1 - \eta_U}\right)^{0.5}_{Cs} \quad .. \quad (12)$$

With this expression, it is possible to estimate the comparative performance of the contact-ionization thrustor

with that of the electron-bombardment thrustor previously described. The durability of the electron-bombardment thrustor is for the overall thrustor module and is limited by the current density at the centre of the accel electrode plate. This current density is about three times the average current density of the module. By applying this correction, it is possible to make a rough estimate of the allowable exhaust-jet power density of a comparable contact-ionization thrustor. The results of this estimate are shown in Fig. 15 for an accel electrode durability of 400 days. If a material with a low
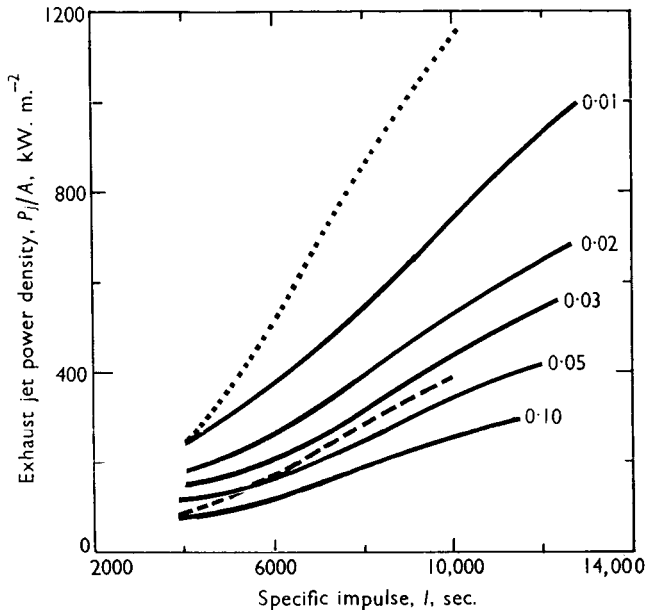

FIG. 15. 400-day durability limits on exhaust-jet power density due to charge-exchange ion erosion of the accel electrode. Contact-ionization thrustor: copper electrode. Electron-bombardment thrustor: molybdenum electrode.

Continuous lines: Contact-ionization thrustor with 2 mm. accel length; neutral atom fractions of from 0·01 to 0·10.

Broken line: Existing electron-bombardment thrustor.

Dotted line: Hypothetical electron-bombardment thrustor with uniform current density profile.

sputtering coefficient could be used for the accel electrode in place of copper in the contact-ionization thrustor, it might be possible to double the power densities shown in Fig. 15. The low power densities shown in Fig. 15 could have a serious adverse effect on thrustor size and specific mass. A similar consequence exists with regard to thrustor efficiency, which will be discussed in the next section.

It should be noted that the calculations presented in Fig. 15 are subject to the accuracy of the assumptions. In charge-exchange ion erosion of the accel electrode, the allowable current density is inversely proportional to the square root of the charge-exchange cross section, charge-exchange region volume, and sputtering yield. This relation tends to reduce the sensitivity of the value of current density to errors in the other parameters. For this reason, the estimate shown in Fig. 15 may be used with a fair confidence.

3. POROUS IONIZER

From the preceding brief discussion and approximate calculations regarding charge exchange, it is clear that low neutral-atom concentration is essential for contact-ionization thrustors. Since the ionizer is responsible for admitting neutral caesium atoms, it is appropriate to examine the status of this component in detail.

Because of the charge-exchange problem, the porous ionizer has been accepted as being superior to solid ionizers (with a reverse flow of fresh neutral atoms passing through the ion beam). In porous ionizers, the caesium vapour flows through the ionizer pores by both Knudsen flow and surface diffusion. If the flow rate due to surface diffusion is greater than that due to Knudsen flow near the pore exist, the predominant fraction of the caesium will flow onto the downstream face of the ionizer, as indicated in Fig. 16. Theoretical
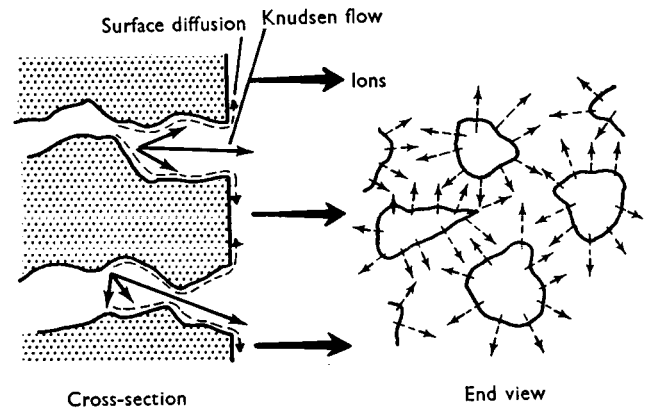

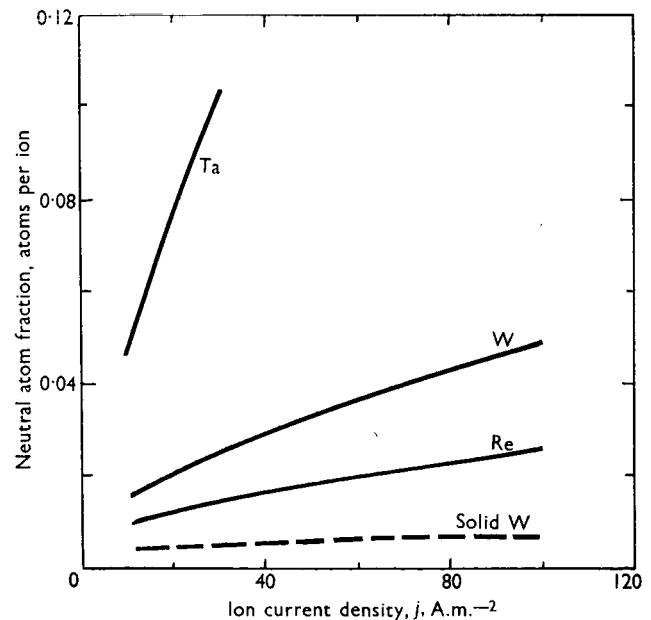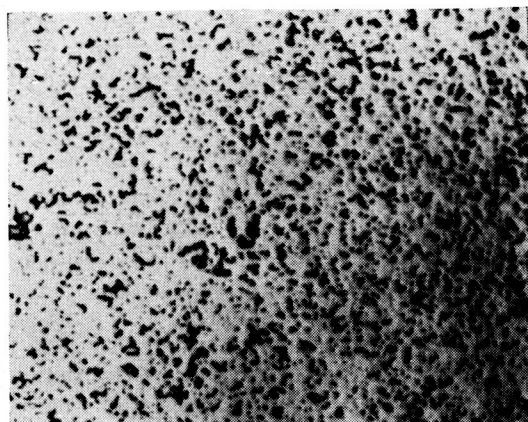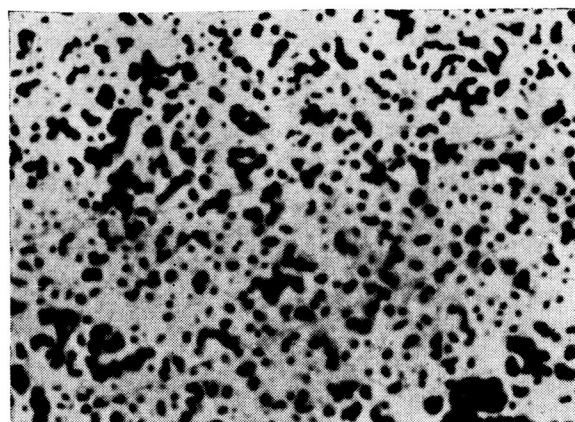FIG. 16. Schematic drawing of flow through porous tungsten.
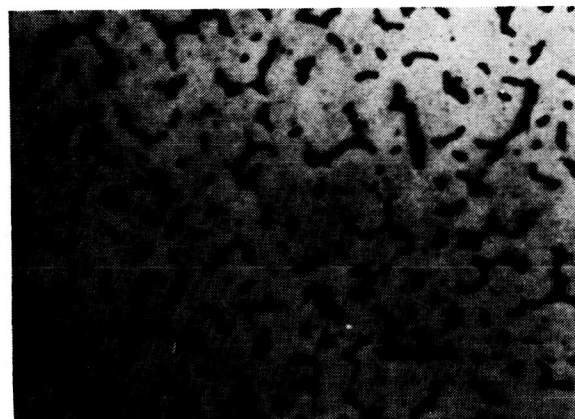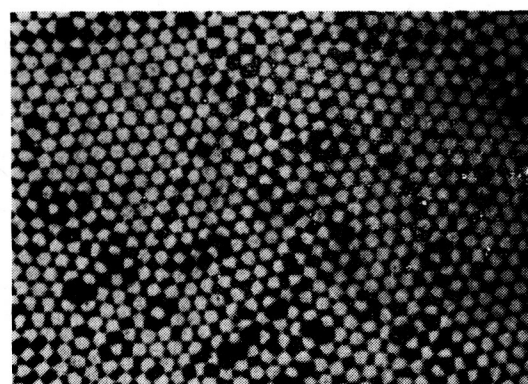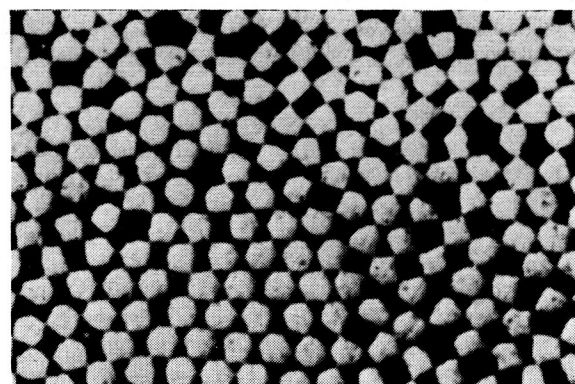

FIG. 17. Neutral-atom efflux from various porous ionizers,
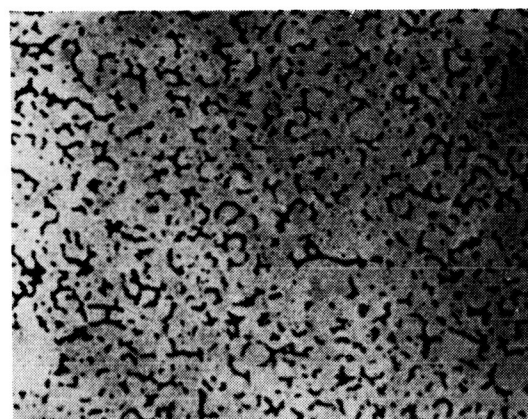
FIG. 18.   Photomicrographs of Electron-Optical Systems, Inc., porous tungsten ionizers.

(*a*) and (*b*): Commercial porous tungsten.
(*c*) and (*d*): Spherical powder.
(*e*) and (*f*): Wire bundle.

analyses of this model of flow and ionization have indicated the need for submicron pore diameters at high ion current densities.[59-61] Experimental results on the neutral-atom efflux from small samples (5 mm. dia.) show that neutral efflux increases as ion current is increased.[62-66] Typical data are shown in Fig. 17, taken from Husman,[64] for a pore size of about 2 μm. and a pore density of 10^6 cm.$^{-2}$ with various porous materials. Porous ionizers with these characteristics are commercially available.

Experimental data recently reported[65] confirm the need for small pore size. Tungsten ionizers made from spherical powder, and others made from wire bundles, were compared with commercial tungsten samples having a 2-μm. pore diameter and 2×10^6 pores per square centimetre. Photomicrographs of these ionizers are shown in Fig. 18. The neutral atom efflux from these ionizers is shown in Fig. 19. It is evident that the spherical-powder tungsten ionizers provide a lower neutral-atom fraction.

To obtain satisfactorily low neutral-atom flux, the pore size must be smaller than at present obtainable, and
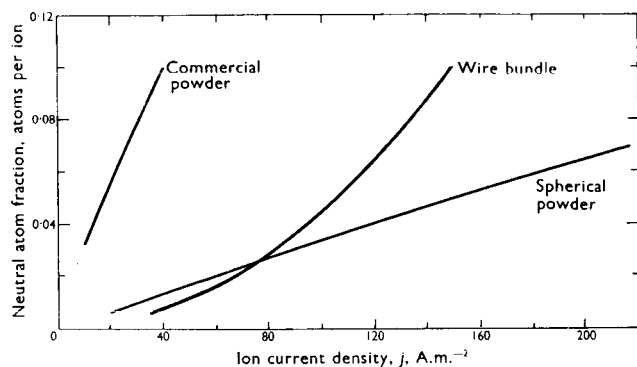
FIG. 19. Neutral-atom efflux from porous tun sten ionizers.

the pore density (number per unit area) must be high, for instance, greater than 3×10^6 cm.$^{-2}$ (Husman[64]). The use of small-diameter tungsten powder would presumably provide these requirements; however, it appears that with small powder diameters, the porous ionizers continue to sinter at the ionizer operating temperature. This sintering fills up the pores and increases the density of the ionizer, resulting in increased neutral-atom efflux that eventually result in cracking due to reduction in volume. At Hughes, several porous-tungsten ionizers with 2- to 4-μm. pores have been operated for 11 months at 1440° K. (Husman[64]). The 4-μm. pore-size ionizers appear to have retained stability over this time, but the 2-μm. pore-size ionizers have suffered substantial increases in flow transmission coefficients. It is possible that this increased flow may indicate the presence of microcracks caused by reduction in volume due to sintering. Thus, small-powder-diameter tungsten ionizers of

the type necessary for low neutral-atom effluxes may sinter shut or crack during the lifetimes required for spaceflight.

In addition to the effect on long-term ionizer sintering, the ionizer temperature is also of great importance to thrustor efficiency, because thermal radiation from the ionizer constitutes the major power loss. In early work on contact ionization, it was found that below a certain critical temperature mostly neutral atoms are evaporated from the surface, while above this temperature mostly ions are emitted. A similar critical temperature is found for porous emitters, although the ion-atom emission does not change as sharply as for solid surfaces. The effect of ionizer temperature on ion current density and neutral-atom fraction is exhibited by typical data from Kuskevics and Thompson[65] shown in Fig. 20. Neutral-atom efflux
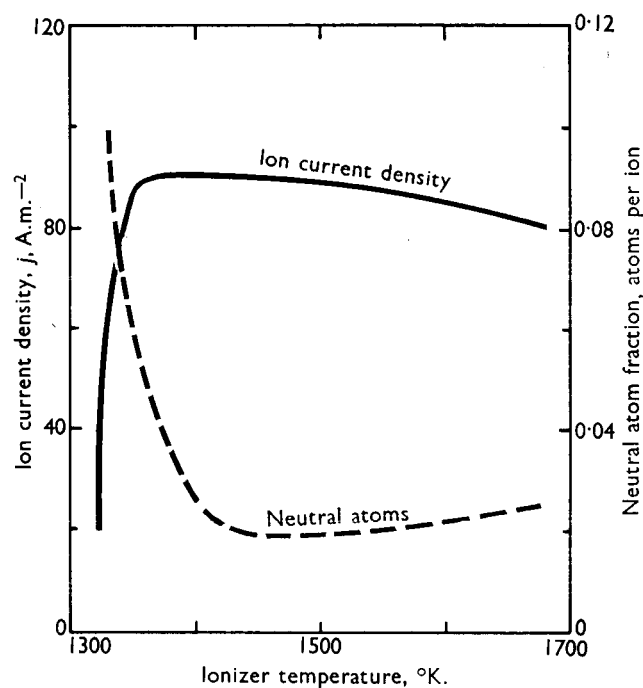
FIG. 20. Effect of ionizer temperature on ion current density and neutral-atom efflux from porous-tungsten ionizer.
Continuous line: Ion current density.
Broken line: Neutral atoms.

minimizes at about 1460° K. (this is the neutral-fraction critical temperature), while the ion critical temperature occurs at about 1360° K. in Fig. 20. Operation at minimal neutral-atom flux would increase the thermal-radiation loss by 37% in this case. Husman's data[64] suggest that smaller pore size and increased pore density could reduce the critical temperatures for ion current and neutral-atom fraction. This is supported by the theoretical analyses.[59-61]

As mentioned in Section V.1, particular thrustor designs may have a non-uniform current density across the ionizer surface. It is evident that the ionizer must be operated at a temperature high enough to accommodate
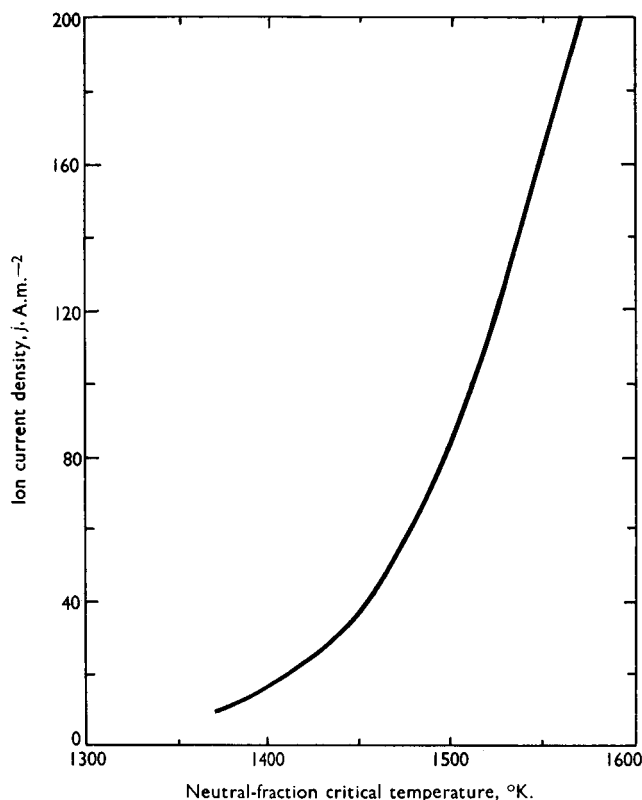
FIG. 21. Neutral-fraction critical temperature for spherical-powder porous-tungsten ionizers.
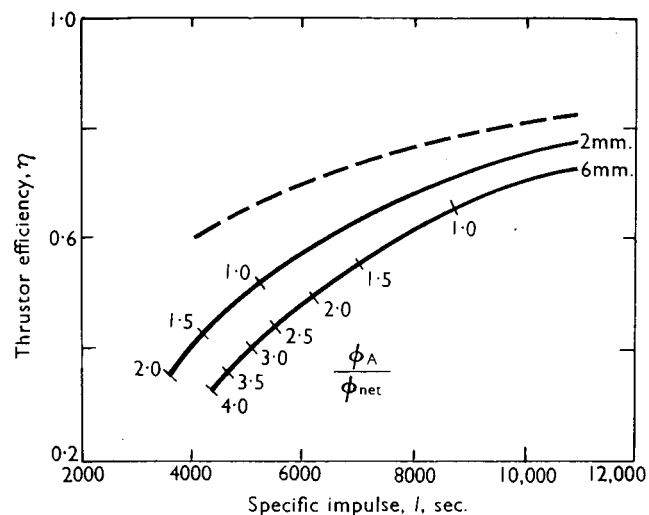

FIG. 22. Estimated limitation on thrustor efficiency due to charge-exchange ion erosion of copper accel electrode. 400-day durability. Spherical-powder porous-tungsten ionizer.

Continuous lines: Hypothetical contact-ionization thrustors of accel length (L) 2 and 6 mm.

Broken line: Existing electron-bombardment thrustor.

the highest local current density. Typical neutral-fraction critical temperatures given[65] for spherical-powder tungsten ionizers are shown in Fig. 21. If the average current density were 60 A.m.$^{-2}$ and a peak existed at 180 A.m.$^{-2}$, the increase in ionizer temperature required to prevent high neutral-atom efflux from the high current spot would result in a 25% increase in thermal-radiation loss.

With the equations presented in Section V.2, it is possible to estimate the maximum thrustor efficiency on the basis of the best existing porous-tungsten characteristics. The spherical powder data from Fig. 19 were used. The emittance of porous ionizers may be subject to surface conditions[64]; so an average value of 0·5 was assumed herein. The heat loss is assumed to be only the thermal radiation from the downstream face of the ionizer. With these assumptions, the estimated maximum efficiency is shown in Fig. 22 together with the present efficiency of the electron-bombardment thrustor. Fig. 22 illustrates the comparatively insensitive nature of this estimate to small errors, with a 3 to 1 difference in accelerator spacing resulting in an 11% efficiency change, or less. Fig. 22 also illustrates the serious shortcomings of present porous-tungsten technology. Without drastic improvements in this technology, present electron-bombardment efficiencies cannot be equalled with long-life contact-ionization thrustors.

A similar estimate of exhaust-jet power density is shown in Fig. 23, which shows that contact-ionization thrustors are about the same size as electron-bombardment thrustors. However, contact-ionization thrustors probably require heavier construction than electron-bombardment thrustors and will not be lighter than those shown in Fig. 10.

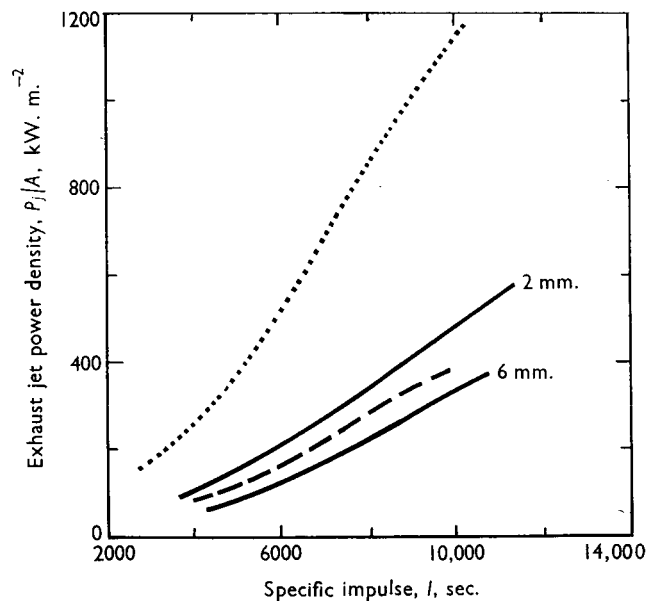FIG. 23. Exhaust-jet power density limitations for hypothetical contact-ionization thrustors with spherical-powder porous-tungsten ionizers and 400-day durability.

Continuous lines: Hypothetical contact-ionization thrustors of accel length (L) 2 and 6 mm.

Broken line: Existing electron-bombardment thrustor.

Dotted line: Hypothetical electron-bombardment thrustor with uniform current-density profile.

The estimates of contact-ionization thrustor perfor-
mance made herein are based on the use of a single set
of accel electrodes. It is evident that if the accel
electrodes could be replaced *en route* with reliable,
light-weight mechanisms, then the allowable current
density would be increased and higher performance
would be possible.

The present efficiencies of EOS and Hughes thrustors
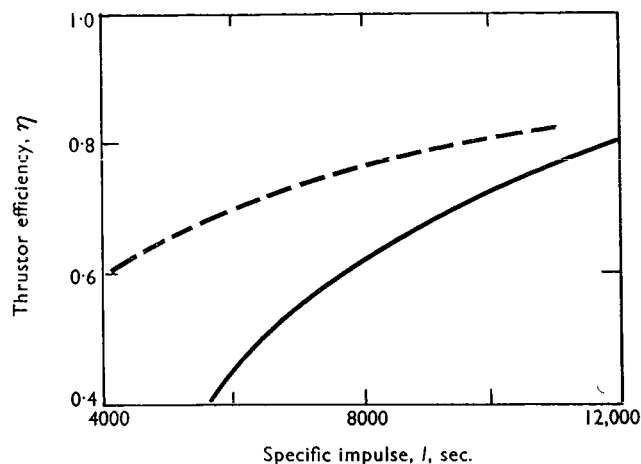(reported by Teem and Brewer[67]) are shown in Fig. 24.

FIG. 24. Efficiency of existing EOS and Hughes contact-ioniza-
tion thrustors, uncorrected for durability (*continuous line*).
Broken line: efficiency of existing electron-bombardment thrustor.

These efficiencies are maxima and are not necessarily
compatible with durability requirements of inter-
planetary missions.

The neutral cæsium atom efflux from porous-tungsten
ionizers can be reduced if uniform submicron pore sizes
and high pore densities (number per unit area) can be
obtained. At the same time, sintering at ionizer operating
temperatures must be slow enough so that the ionizer
has a durability of at least 400 days. This ionizer prob-
lem has been recognized for a number of years, and
many man-years of applied research have been devoted
to ionizer improvement. In spite of this effort, satis-
factory porous-tungsten ionizers have not yet been
developed.

A number of possible research avenues have been dis-
cussed by Anglin.[68] These avenues are, in one form or
another, now under investigation in a number of
laboratories.

Other geometries also offer some hope of improved
performance for contact-ionization thrustors. Examina-
tion of Fig. 14 shows that charge-exchange impingement
results primarily from charge-exchange processes near
the accelerator, with those occurring near the ionizer
being relatively unimportant. A divergent-flow
thrustor,[69] such as that illustrated in Fig. 25, would have
a high current density at the ionizer to decrease the heat
loss, but a low current density near the accelerator, where
most of the erosion effects originate. Calculations for a
divergent-flow thrustor (with an area ratio of 2 between
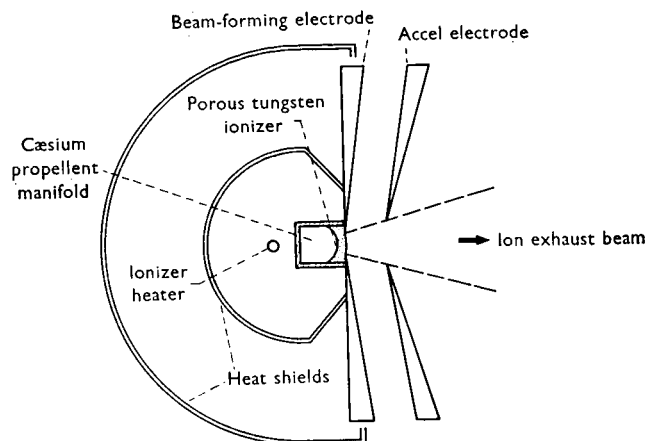
FIG. 25. Divergent-flow contact-ionization thrustor designed at
the N.A.S.A. Lewis Laboratory. Ionizer height, 101 mm.;
ionizer chord, 1·5 mm.; ionizer radius, 3 mm.; exhaust aperture
radius, 6 mm.

the ionizer and the beam at the accelerator aperture)
indicate that efficiencies slightly better than those of
present electron-bombardment thrustors might be
achieved with present porous-tungsten technology.

Perhaps the lower neutral fractions and heat losses of
solid-tungsten ionizers would even justify a return to
the reverse-feed concept previously investigated.[70-72] If
the neutral cæsium were introduced close to the ionizer,
as indicated in Fig. 26, the charge exchange would be
substantially restricted to the "safe" region near the
ionizer.
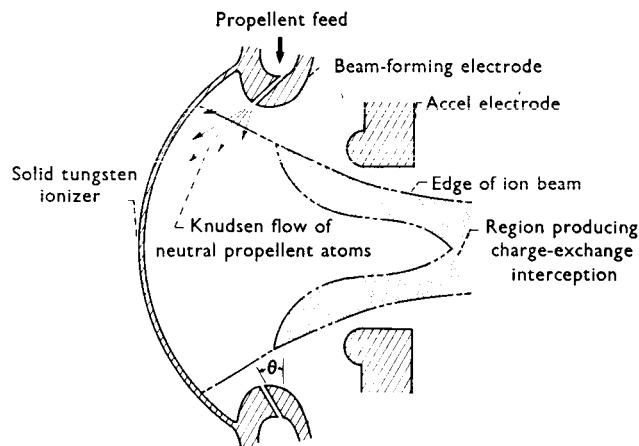
FIG. 26. Hypothetical design for reverse-feed contact-ionization
thrustor.

VI. COLLOIDAL-PARTICLE THRUSTORS

Complete colloidal-particle thrustors do not exist at
present. Devices have been operated in which colloidal
particles are generated, charged, and accelerated; but
these are only preliminary experiments and do not qualify
as thrustors. The purpose of this section is to review
and evaluate experimental work on potential colloidal-
particle thrustor components.

The motivation for colloidal-particle research is similar to that for heavy molecules. By increasing the particly mass, the ratio of kinetic energy to charging energe should increase at any given exhaust velocity, thus raising the efficiency. This increase in efficiency is most needed in the lower range of specific impulses, so the generation of particles should be examined with a view to their use at these lower values. A number of particle generation schemes are now being investigated. The minimum mean mass-to-charge ratio m/q that has been obtained experimentally with each of these methods is given in Table I.

TABLE I.

Method	Minimum mean m/q, amu/Ze	Reference
Ion nucleation	1,400,000	73
Preformed (agglomerated) solid ..	950,000	74
Liquid drops from sprays	480,000	75, 76
	14,000,000	77, 78
Surface condensation	700,000	79
Vapour condensation	100,000	80, 81

If a specific impulse of 5000 sec. with a net accelerating potential difference less than 100 kV. is considered, then the maximum usable m/q should be about 8000 amu/Ze. Even if the potential difference were raised to 10^6 V. the maximum usable m/q would be below the values shown in the preceding table. Although work in this field has been going on for several years, the total research effort has been small.

Research is continuing on each of the above methods in an effort to provide the proper m/q range with good utilization efficiency.

1. ION NUCLEATION

In the ion-nucleation method[73] a supersaturated vapour stream is partly ionized. The ions are intended to be condensation nuclei. By applying a retarding electric field, the nuclei are slowed down to provide enough time for particle growth. Charged particles with a large enough m/q would pass over the retarding potential difference, so that a supply of particles with uniform m/q would result. This method is still in the basic research stage.

2. PREFORMED PARTICLES

Preformed solid particles with a mean size of 70 Å. have been gravity fed through ducts to an electron-bombardment ionization chamber, ionized, acclerated, and analyzed for charge/mass distribution.[74] The particles were initially agglomerated and remain partly agglomerated through the charging process. However, the mass/charge ratio was only about a decade too high, so this experiment provides some evidence that the use of preformed solid particles might be possible.

3. ELECTRIC SPRAYING

A major share of the colloidal-particle-thrustor research has been devoted to particle generation and simultaneous charging of electrically sprayed liquid droplets. The drops are formed and charged at sharp hollow needle points[75-78] or at a sharp edge of a spinning cup[82] with a high electric field at the point or edge. Drop formation occurs by a combination of fluid instability and dielectrophoresis.[75,76] Charging occurs at the instant of separation from the tip by charge transfer.

The electric field strength must be high at the tip in order to obtain small drop sizes. If the field strength is too high, a glow discharge occurs that generates a large ion current. This ion current may cause a serious power loss in the acclerator. Recent experiments have shown that the electric spraying process may be sporadic.[77] At first, the liquid tip is sharp, and small charged drops are emitted. Then the liquid tip builds up and a very large charged drop is emitted accompanied by many ions. These sequences are sporadically repetitive. These data also show a very wide range of m/q.

The high-speed photomicrographic data[77] indicate that if the liquid is conducting, the electric field penetrates the bulging liquid drop at the tip, preventing the formation of small drops. If the liquid is nonconducting, the high field strength is preserved, but a finite time is required to accumulate a charge in the "liquid tip." This low rate of charge accumulation limits the mass flow rate of liquid from each hollow needle. For example, a maximum of 1 μA. per needle has been quoted.[75] If the net accelerating voltage were 10^6 V., there would be 1 W. of thrustor exhaust power per needle. From the preceding sections it is evident that an exhaust power desity of 100 kW.m.$^{-2}$ is required in order to be comparable in size with the existing electron-bombardment thrustor at 5000 sec. At an exhaust power density of 100 kW.m.$^{-2}$, 10^5 needles would be required per square metre. The needle spacing would be 3 mm. It seems reasonable to expect that such a needle density would lower the electric field strength at each needle tip, perhaps below that required for electric spraying.

The charge-accumulation limit also appears pertinent to the surface-condensation scheme. In fact, the literature does not contain even approximate analyses to demonstrate that the electric-spraying or surface-condensation schemes might be useful in real electrostatic thrustors.

4. VAPOUR CONDENSATION

To date, the vapour-condensation method has not only produced values of m/q approaching the range of interest for propulsion[80] but has also been incorporated in a laboratory device that has produced a substantial thrust.[81] In this method of particle generation, a supersaturated vapour enters a condensation shock wave where

particle nucleation occurs. Subsequent growth is controlled by the flow conditions. The colloidal particles are then charged by electron attachment in a glow discharge. Particle size distributions have been measured for a number of propellents, such as $AlCl_3$, $HgCl_2$ and $HgCl$. Ion currents have not been observed. The fraction of total propellent that is converted into colloidal particles has yet to be determined.

The vapour-condensation method[80,81] is being investigated at Lewis in apparatus resembling a real thrustor. The past experiments have been made with a 50,000-V. power supply, but a 150,000-V. facility is now available, and a 400,000-V. facility is under construction. With such high-voltage power available, a greatly improved evaluation of this thrustor concept will be possible.

Quadrupole and monopole massenfilters (mass spectrometers) are being developed at Lewis for measurement of particle mass charge in the exhaust beam from experimental thrustors. With measurements of particle mass/charge, thrust, beam current, particle size and total propellent mass flow rate, it is expected that an accurate determination of propellent utilization can be made.

Fundamental studies of particle nucleation and growth are being made at Lewis. It is hoped that such studies will aid in the design of particle generator nozzles that will provide particles with a mass of less than 100,000 amu and with the narrow size distribution, which is necessary for good accelerator efficiency. In addition to the electron-attachment method of particle charging, several other methods are under investigation, which include electron bombardment, field emission and photo-ionization.

VII. CONCLUDING REMARKS

With the exception of the cathode, the electron-bombardment thrustor is capable of durabilities required for interplanetary round-trip missions. Experimental results from recent cathode tests indicate that alkaline-earth carbonate coatings may provide adequate durability at acceptable heater-power levels. It is also expected that the autocathode version of the electron-bombardment thrustor will have adequate durability. It is difficult to foresee any substantial improvement in the efficiency of the electron-bombardment thrustor. Although serious payload losses would be incurred with the electron-bombardment thrustor, it could be used for most electric-propulsion missions in its present form.

The ionizer in the contact-ionization thrustor is not adequate at present because of the inability to produce porous tungsten with sufficiently low neutral-atom loss and simultaneously to prevent unacceptable in-flight-sintering rates. Because of the high neutral-atom loss from porous tungsten ionizers, charge-exchange ion erosion of electrodes places a severe limit on contact-ionization thrustor efficiency, particularly in the lower range of specific impulse. The problems of porous tungsten ionizers—unless modified by substantial improvements in technology—are formidable enough to prevent the use of contact-ionization thrustors for primary propulsions.

Colloidal-particle thrustors do not exist at present. With the exception of the vapour-condensation method, existing methods of colloidal-particle generation produce particles with much too high a mass/charge ratio. At present, the vapour-condensation method would require accelerator voltages of 400,000 V. to obtain a specific impulse of 3000 sec., which is near the lowest value of interest. Not enough is known at present to predict accurately the ultimate performance of the colloidal-particle thrustor.

Comparisons between electrostatic, electrothermal and electromagnetic (plasma) thrustors have been avoided. Mission analyses show that the specific impulse of electrothermal thrustors is well below the range of interest for interplanetary missions. Existing plasma thrustors have unacceptably low efficiencies, and there is no concrete evidence at present on which to base estimates of future performance.

The development of moderately efficient thrustors, with excellent prospects of reaching desired lifetimes with further work, has served to highlight the shortcomings of electric propulsion as a system. The need for efficient, lightweight, reliable electric power sources and power-conversion equipment is particularly obvious.

REFERENCES

1. J. C. Evvard, *Astronautics aerospace Engng*, Aug., 1963, 1 (7), 92.
2. W. E. Moeckel, "Electric Propulsion Systems for Mars Missions," *Paper presented at Symposium on the Exploration of Mars, Denver, Colorado, 6–7 June,* **1963**.
3. L. Schipper, R. S. Siegler and E. B. Zwick, "Advanced 1-Megawatt Space Power Plant Study," *Am. Inst. Aeronaut. Astronaut. Pap.,* 1963 (63-270).
4. D. T. Bernatowicz, *ARS J.,* 1962, **32**, 1256.
5. D. G. Elliot, *ibid.,* 924; also as *NASA JPL tech. Rep.,* 1962 (32-116).
6. B. H. Beam, "An Exploratory Study of Thermoelectric Power Generation for Space Flight Applications," *NASA tech. Note,* 1960 (TN D-336).
7. A. L. Cox, "Colloidal Electrohydrodynamic Energy Converter," *Am. rocket Soc. Pap.,* 1962 (2559-62).
8. G. W. Englert, "Study of Thermonuclear Propulsion Using Superconducting Magnets," *Paper presented at Third a. Conf. Engng Magnetohydrodynamics, Rochester, N.Y.,* March, **1962**.
9. W. R. Mickelsen and C. A. Low, Jnr., *Astronautics aerospace Engng,* Oct., 1963, 1 (9), 52.
10. W. R. Mickelsen and H. R. Kaufman, "Status of Electrostatic Thrustors for Space Propulsion," *NASA tech. Note,* 1964 (TN D-2172).
11. J. H. Irving and E. K. Blum, "Vistas in Astronautics, Vol. 2" (edited by M. Alperin and H. F. Gregory), p. 191. **1959**: London (Pergamon).
12. W. G. Melbourne, "Interplanetary Trajectories and Payload Capabilities of Advanced Propulsion Vehicles," *NASA JPL tech. Rep.,* March, 1961 (32-68).
13. C. G. Sauer, Jnr., and W. G. Melbourne, "Optimum Earth-to-Mars Roundtrip Trajectories Utilizing a Low-Thrust Power-Limited Propulsion System," *Paper presented at Ninth a. Meet. am. astronaut. Soc., Los Angeles,* Jan., **1963**.
14. J. S. MacKay. Unpublished analyses. NASA Lewis Research Center, Cleveland, Ohio.

*15. Aerospace Electrical Division, Westinghouse Electric Corp., Lima, Ohio, "Space Electric Power Systems Study: Fourth Quarter Progress Report, NASA Contract NAS 5-1234," Nov., **1962**.

16. C. S. Corcoran, Jnr., Unpublished analysis. NASA Lewis Research Center, **1963**.

17. H. R. Kaufman, "One-Dimensional Analysis of Ion Rockets," *NASA tech. Note*, 1960 (TN D-261).

18. H. Mirels and B. M. Rosenbaum, "Analysis of One-Dimensional Ion Rocket with Grid Neutralization," *NASA tech. Note*, 1960 (TN D-266).

19. H. R. Kaufman, "The Neutralization of Ion-Rocket Beams," *NASA tech. Note*, 1961 (TN D-1055).

20. J. M. Sellen and R. F. Kemp, "Cesium Ion Beam Neutralization in Vehicular Simulation," *Am. rocket Soc. Pap.*, 1961 (**61-84-1778**).

21. J. H. Childs and R. J. Cybulski, "Flight Tests and Early Missions for Electric Propulsion Systems," *Am. rocket Soc. Pap.*, 1962 (**2653-62**).

22. R. F. Kemp, J. M. Sellen and E. V. Pawlik, "Neutralizer Tests on a Flight-Model Electron-Bombardment Ion Thrustor," *NASA tech. Note*, 1963 (TN D-1733).

23. M. Von Ardenne, "New Developments in Applied Ion and Nuclear Physics," *Atomic Energy Res. Establishment Library Translation*, 1957 (**758**).

24. H. R. Kaufman and P. D. Reader, "Experimental Performance of Ion Rockets Employing Electron-Bombardment Ion Sources," *Am. rocket Soc. Pap.*, 1960 (**1374-60**).

25. H. R. Kaufman, "An Ion Rocket with an Electron-Bombardment Ion Source," *NASA tech. Note*, 1961 (TN D-585).

26. D. B. Langmuir, E. Stuhlinger and J. M. Sellen, Jnr. (Editors), "Progress in Astronautics and Rocketry. Vol. 5. Electrostatic Propulsion." **1961**: New York (Academic Press).

27. R. C. Speiser and L. K. Branson, "Studies of a Gas Discharge Cesium Ion Source," *Am. rocket Soc. Pap.*, 1962 (**2664-62**).

*28. W. Sirois, "Cathode Development Studies for Arc and Bombardment-Type Ion Engines: Final Summary Report for NASA Contract NAS 8-2513," *Ion Physics Corp. Rep.*, April, **1963**.

*29. J. Hyman, Jnr., C. R. Buckey, W. O. Eckhardt, and R. C. Knechtli, "Research Investigation of Ion Beam Formation from Electron-Bombardment Ion Sources: Interim Technical Report on Completion of Phase I, NASA Contract NAS 3-2511," *Hughes res. Labs Rep.*, April, **1963**.

30. P. D. Reader, "Investigation of a 10-Centimeter-Diameter Electron-Bombardment Ion Rocket," *NASA tech. Note*, 1962 (TN D-1163).

31. N. L. Milder, "Comparative Measurements of Singly and Doubly Ionized Mercury Produced by Electron-Bombardment Ion Engine," *NASA tech. Note*, 1962 (TN D-1219).

32. W. R. Mickelsen, "NASA Research on Heavy-Particle Electrostatic Thrustors," *Inst. aerospace Sci. Pap.*, 1963 (**63-19**).

33. P. D. Reader, "An Electron-Bombardment Ion Rocket with a Permanent Magnet," *Am. Inst. Aeronaut. Astronaut. Pap.*, 1963 (**63031**), *AIAA J.*, in the press.

34. N. L. Milder and W. R. Kerslake, "High-Temperature Metal Filaments for Electron-Bombardment Ion Sources." Proposed *NASA tech. Note*.

35. H. R. Kaufman, "The Electron-Bombardment Ion Rocket," *Paper presented at AFOSR Third Symp. advd Propulsion Concepts, Cincinnati, Ohio*, 2-4 October, **1962**.

36. W. R. Kerslake, "Accelerator Grid Tests on an Electron-Bombardment Ion Rocket," *NASA tech. Note*, 1962 (TN D-1168).

37. W. R. Kerslake and E. V. Pawlik, "Additional Studies of Screen and Accelerator Grids for Electron-Bombardment Ion Thrustors," *NASA tech. Note*, 1963 (TN D-1411).

38. W. R. Kerslake, "Charge-Exchange Effects on the Accelerator Impingement of an Electron-Bombardment Ion Rocket," *NASA tech. Note*, 1963 (TN D-1657).

39. R. C. Speiser and R. H. Vernon, "Cesium Ion-Atom Charge Exchange Scattering," *Am. rocket Soc. Pap.*, 1961 (**2068-61**).

40. G. Kuskevics, R. C. Speiser, R. M. Worlock and D. Zuccaro, "Ionization, Emission, and Collision Processes in the Cesium Ion Engine," *Am. rocket Soc. Pap.*, 1962 (**2364-62**).

41. E. Stuhlinger, *Internat. astronaut. Congr., Proc. Vth Congr.*, 1954, p. 100.

42. E. Stuhlinger, *J. Astronautics*, 1955, **2**, 149; ibid., 1956, **3**, 11, 33.

43. S. Naiditch, R. M. Worlock, D. Zuccaro, D. Baker, M. P. Ernstene, L. R. Gallagher and J. Mullins, "Ion Propulsion Systems: Experimental Studies," *Am. rocket Soc. Pap.*, 1959 (**928-59**).

44. C. R. Dulgeroff, R. C. Speiser and A. T. Forrester, "Experimental Studies with Small Scale Ion Motors," *Am. rocket Soc. Pap.*, 1959 (**926-59**).

45. M. P. Ernstene, A. T. Forrester, R. C. Speiser and R. M. Worlock, "Multiple Beam Ion Motors," *Am. rocket Soc. Pap.*, 1960 (**1373-60**).

46. M. P. Ernstene, A. T. Forrester, E. L. James, D. Telel and R. M. Worlock, "Development of High Efficiency Cesium Ion Engines," *Am. rocket Soc. Pap.*, 1961 (**61-83-1777**).

47. R. S. H. Toms, M. P. Ernstene, B. E. Kalensher and G. R. Selg, "Space Testing of Ion Engines," *Am. rocket Soc. Pap.*, 1961 (**2182-61**).

48. J. E. Densmore, R. R. Tanquay and B. M. Wilner, "Development of Ion Thrustor Systems for Space Flight Testing," *Am. rocket Soc. Pap.*, 1962 (**2369-62**).

49. G. R. Brewer, J. E. Etter and J. R. Anderson, "Design and Performance of Small Ion Engines," *Am. rocket Soc. Pap.*, 1960 (**1125-60**).

50. J. E. Etter, S. L. Eilenberg, J. R. Anderson, J. W. Ward and G. R. Brewer, "The Development of a Flight Test Ion Engine," *Am. rocket Soc. Pap.*, 1961 (**61-81-1775**).

51. G. R. Brewer and G. A. Work, "An Ion Engine System for Flight Testing," *Am. Inst. electl Engrs Conf. Pap.* 1962 (**CP62-1162**).

52. R. A. Hubach, "Limitations on the Space Test of a Cesium Ion Engine at Altitudes below 1500 Kilometers," *Am. rocket Soc. Pap.*, 1962 (**2366-62**).

53. M. D. Stribling and J. E. Etter, "Recent Results on the Development of Cesium Ion Engines," *Am. Inst. Aeronaut. Astronaut. Pap.*, 1962 (**2366-62**).

54. D. L. Lockwood and V. Hamza, "Space-Charge Flow Theory and Electrode Design for Electrostatic Rocket Engines," *NASA tech. Note*, 1962 (TN D-1461).

55. V. Hamza and E. A. Richley, "Numerical Solution of Two-Dimensional Poisson Equation: Theory and Application to Electrostatic-Ion-Engine Analysis," *NASA tech. Note*, 1963 (TN D-1323).

56. V. Hamza, "Numerical Solution of Axially-Symmetric Poisson Equation: Theory and Application to Ion-Thrustor Analysis," *NASA tech. Note*, 1963 (TN D-1711).

57. J. F. Wasserbauer, "Experimental Performance of a High Current Density Cylindrical Concave Porous Tungsten Emitter for Ion Engines," *Am. Inst. Aeronaut. Astronaut. Pap.*, 1963 (**63029**).

58. T. W. Reynolds and E. A. Richley, "Thermionic Emission from Cesium-Coated Electrostatic Ion-Thrustor Electrodes," *NASA tech. Note*, 1963 (TN D-1879).

59. G. M. Nazarian and H. Shelton, "Theory of Ion Emission from Porous Media," *Am. rocket Soc. Pap.*, 1960 (**1386-60**).

60. D. Zuccaro, R. C. Speiser and J. M. Teem, "Characteristics of Porous Surface Ionizers," *Am. rocket Soc. Pap.*, 1960 (**1387-60**).

61. T. W. Reynolds and L. W. Kreps, "Gas Flow, Emittance, and Ion Current Capabilities of Porous Tungsten," *NASA tech. Note*, 1961 (TN D-871).

62. O. K. Husman, "Experimental Evaluation of Porous Materials for Surface Ionization of Cesium and Potassium," *Am. rocket Soc. Pap.*, 1962 (**2359-62**).

63. H. Shelton, "Experiments on Atom and Ion Emission from Porous Tungsten," *Am. rocket Soc. Pap.*, 1962 (**2360-62**).

64. D. K. Husman, "A Comparison of the Contact Ionization of Cesium on Tungsten with that of Molybdenum, Tantalum, and Rhenium Surfaces," *Am. Inst. Aeronaut. Astronaut. Pap.*, 1963 (**63019**).

65. G. Kuskevics and B. L. Thompson, "Comparison of Commercial, Spherical Powder and Wire Bundle Tungsten Ionizers," *Am. Inst. Aeronaut. Astronaut. Pap.*, 1963 (**63016**).

66. R. G. Wilson, G. D. Seele and J. F. Hon, "Surface Ionization of Cesium with Porous Tungsten Ionizers," *Am. Inst. Aeronaut. Astronaut. Pap.*, 1963 (**63017**).

67. J. M. Teem and G. R. Brewer, "Current Status and Prospects of Ion Propulsion," *Am. rocket Soc. Pap.*, 1962 (**2650-62**).

68. A. E. Anglin, Jnr., "Problems of Porous Tungsten Ionizers for Cesium Electric Propulsion Systems," *Pap. presented at nat. Soc. aerospace process Engrs, Spring Symp. on Space Power Systems Mater., Philadelphia, Pa.*, 3–5 June, **1963**.

69. W. R. Mickelsen, "Theoretical Performance of Electrostatic Thrustors with Analytic Space-Charge Flows," *NASA tech. Rep.*, 1963 (**TR R-174**).

70. E. E. Dangle and D. L. Lockwood, "NASA Experimental Research with Ion Rockets," *Am. rocket Soc. Pap.*, 1960 (**1126-60**).

71. J. H. Childs, "Theoretical Performance of Reverse-Feed Cesium Ion Engines," *NASA tech. Note*, 1961 (**TN D-876**).

72. T. W. Reynolds and J. H. Childs, "A Comparison of Reverse-Feed and Porous-Tungsten Ion Engines," *NASA tech. Note*, 1962 (**TN D-1166**).

73. A. L. Cox and S. Harrison, "The Controlled-Growth Colloidal Ion Source," *Am. Inst. Aeronaut. Astronaut. Pap.*, 1963 (**63049**).

74. S. Singer, N. G. Kim and M. Farber, "An Experimental Study of Colloidal Propulsion Using Sub-Micron Particles," *Am. Inst. Aeronaut. Astronaut. Pap.*, 1963 (**63052**).

75. V. E. Krohn, Jnr., "Liquid Metal Drops for Heavy Particle Propulsion," *Am. rocket Soc. Pap.*, 1960 (**1375-60**).

76. V. E. Krohn, Jnr., "Glycerol Droplets for Electrostatic Propulsion," *Am. rocket Soc. Pap.*, 1962 (**2398-62**).

77. C. D. Hendricks, Jnr., R. S. Carson, J. J. Hogan and J. M. Schneider, "Photomicrography of Electrically Sprayed Heavy Particles," *Am. Inst. Aeronaut. Astronaut. Pap.*, 1963 (**63051**).

78. C. D. Hendricks, "Physics of Charged Colloidal Particles and the Technology of Their Production," *Pap. presented at AGARD Combust. Propulsion Panel, Athens, Greece*, 15–17 July, **1963**.

79. D. M. Jamba and B. Hornstein, "Charging and Removal of Surface-Condensed Particles for Colloid Propulsion," *Am. Inst. Aeronaut. Astronaut. Pap.*, 1963 (**63053**).

80. C. T. Norgren, "Onboard Colloidal Particle Generator for Electrostatic Engines," *Am. rocket Soc. Pap.*, 1962 (**2380-62**).

81. D. S. Goldin and C. T. Norgren, "Thrust Measurements of Colloidal Particles as an Indication of Particle Size and Thrustor Operation," *Am. Inst. Aeronaut. Astronaut. Pap.*, 1963 (**63050**).

*82. D. Gignoux, H. Einbinder and H. Anton, "Nozzle for Colloidal Propulsion: Analytical Investigation: Final Report, Phase I, NASA Contract No. NASr-45, Cosmic, Inc., August, **1961**.